PHYSICAL REVIEW B VOLUME 27, NUMBER 3 1 FEBRUARY 1983

Phase diagram of one-dimensional electron-phonon systems. I. The Su-Schrieffer-Heeger model

Eduardo Fradkin
Department of Physics, University of Illinois at Urbana-Champaign, Urbana, Illinois 61801 and Institute for Theoretical Physics, University of California, Santa Barbara, California 93106*

Jorge E. Hirsch†
Institute for Theoretical Physics, University of California, Santa Barbara, California 93106
(Received 19 July 1982)

We study the nature of the ground state of the Su-Schrieffer-Heeger model for electron-phonon interactions in one dimension in the half-filled-band case. We consider the cases of spinless electrons ($n=1$) and spin-$\frac{1}{2}$ electrons ($n=2$), and discuss the stability of the Peierls-dimerized ground state as a function of the ionic mass and electron-phonon coupling constant. We first consider the zero-mass limit of the theory and extend our results to finite mass using renormalization-group arguments. For spinless electrons, it is found that quantum fluctuations destroy the long-range dimerization order for the small electron-phonon coupling constant if the ionic mass is finite. For spin-$\frac{1}{2}$ electrons, the system is dimerized for an arbitrary coupling constant and phonon frequency. Renormalization-group trajectories show that the low-energy behavior of the system is governed by the zero-mass limit of the theory, an n-component Gross-Neveu model. Monte Carlo simulations are performed for the model at finite phonon frequencies, and the results are compared with the static limit result. We study in particular the set of parameters appropriate for polyacetylene and find a 15% reduction in the phonon order parameter due to fluctuations of the phonon field. A finite-size scaling analysis of the numerical data for the cases $n=1$ and 2 is performed, which confirms the results obtained from the renormalization-group analysis.

I. INTRODUCTION

In recent years one-dimensional electron-phonon systems have attracted renewed attention. In their study of the properties of quasi-one-dimensional systems like polyacetylene, Su, Schrieffer, and Heeger[1] (SSH) introduced a model in which the phonons interact with the electrons by modifying the electron hopping matrix elements. Working with the assumption that the phonon degrees of freedom may be treated classically, since the ionic mass M is very large, SSH further studied the system within the mean-field adiabatic approximation. The resulting physics turned out to be quite rich. The system, for a half-filled band, undergoes a Peierls instability and the ground state is dimerized. SSH also considered the spectrum of low-lying excitation,[2] in particular the soliton states, soliton-fermion bound states, etc. Takayama, Lin-Liu, and Maki[3] introduced a continuum version of the SSH model and studied it in the same approximation as SSH. More recently Nakahara and Maki[4] considered the first quantum corrections to the adiabatic approximation and Campbell and Bishop[5] studied its semiclassical static limit.

In this paper we study the behavior of this one-dimensional electron-phonon system for all values of the ionic mass M and the electron-phonon coupling constant g in the half-filled band case. In particular we want to address the question of whether the dimerized ground state is stable against fluctuations of the phonon field. Furthermore, we want to study the dependence of the results on the number of components of the electron spin. In the adiabatic limit the electronic spin appears to play no significant role, unlike what happens in systems with local four-fermion interactions like the Hubbard model. However, we will see that spin fluctuations also play an important role in systems like the SSH model when the quantum fluctuations of the phonon field are taken into consideration.

The understanding of coupled electron-phonon

systems for all values of M and g is a very difficult problem. However, one may gain considerable insight into the stability problem by simply considering limiting situations. By analyzing the stability of these limits a qualitative picture of the possible phases (or ground states) of the system will emerge. When doing so we will use renormalization-group ideas to extrapolate away from these limits. It is important to note that this procedure provides not only the ground-state properties but also the low-lying spectrum. Furthermore, we do a numerical study of the model using recently developed Monte Carlo techniques,[6] which can give us information also outside of the region where the theoretical treatment is expected to be valid.

We consider the SSH model and two cases are studied: (a) spinless electrons ($n=1$) and (b) spin-$\frac{1}{2}$ electrons ($n=2$), n being the number of spin states. In a subsequent paper we study the molecular crystal model for electron-phonon interactions[7] using similar techniques. In these models there are only two free parameters: the ion's mass M and the electron-phonon coupling constant g. We consider limiting cases in the M-g plane and nontrivial effective Hamiltonians are constructed. The continuum version of the models is considered and compared with the lattice version.

Previous work has concentrated on the large-M behavior of the theory.[1-4] In this paper emphasis is put on the opposite limit, $M=0$. We will show that the long-distance, low-energy behavior of the theory for finite M is governed by the $M=0$ limit, which is an n-component Gross-Neveu (GN) model.[8] As in the GN model, we find that for $n>2$ the system has long-range dimerization order for abitrary coupling. The underlying reason is that the phonon fluctuations induced an effective electron-electron interaction which has no attractive forward scattering component. The umklapp scattering opens up a gap in the electronic spectrum for $n\geq 2$ and gives long-range dimerization order. In contrast, for $n=1$ the umklapp scattering is not effective in opening up a gap for the small coupling constant because of the Pauli exclusion principle. Consequently, we find that the $n=1$ model has a disordered phase for a small electron-phonon coupling constant if the mass of the ions is finite. As the mass of the ions goes to infinity, the size of the disordered region shrinks to zero. The numerical study using the Monte Carlo method allows us to get quantitative results for various lattice and electronic properties for essentially arbitrary parameters. We study, in particular, the set of parameters appropriate for polyacetylene, and find a 15% reduction in the order parameter due to phonon fluctuations. The optical-phonon frequency is found to be reduced by a factor of 0.64. To extract the asymptotic behavior of the model, we perform a finite-size scaling analysis of the numerical data for a case of large ionic frequency. We also do the corresponding analysis for the case $M=\infty$, as a check on our procedure. For the case $n=2$, our analysis shows the behavior expected in the Gross-Neveu model for a small coupling constant and the crossover towards static behavior as the coupling constant increases. For the case $n=1$, our numerical data show a transition for a finite coupling constant in accordance with the theoretical analysis.

The case $n=1$ could be of interest for systems with small values of the gap, where a strong enough magnetic field can be applied that effectively decouples the spin-up and spin-down electrons. It is also of interest in connection with the spin-Peierls transition. Our model with $n=1$ is equivalent, through a Jordan-Wigner transformation, to an xy spin chain that undergoes a spin-Peierls transition.[9] In the future it will be of interest to study the corresponding problem for the Heisenberg chain, which amounts to adding a nearest-neighbor repulsion term to the spinless fermion Hamiltonian. Further extensions of this work will include a study of the behavior of the model in the presence of a magnetic field, extension to non-half-filled band cases, and inclusion of electron-electron interactions.

The paper is organized as follows. In Sec. II the model is defined, and the phase diagrams as well as the low-lying spectra are worked out. We will restrict ourselves to the half-filled-band case at zero temperature. In Sec. III we present results of numerical simulations for the cases $n=2$ and 1 and various sets of parameters, as well as a finite-size scaling analysis of the numerical data. Part of the results presented in this paper were reported briefly elsewhere.[10]

II. MODEL AND PHASE DIAGRAMS

The SSH Hamiltonian[1] is defined as

$$H_{\mathrm{SSH}}=-t\sum_{j,s}(C_{j,s}^{\dagger}C_{j+1,s}+\mathrm{H.c.})-\alpha\sum_{j,s}(q_j-q_{j+1})(C_{j,s}^{\dagger}C_{j+1,s}+\mathrm{H.c.})+\sum_j\left[\frac{P_j^2}{2M}+\frac{D}{2}(q_j-q_{j+1})^2\right], \quad (2.1)$$

where D is the elastic constant and $s=1,\ldots,n$ are the spin components. j runs from 1 to N, the number of lattice sites, and we will be interested in the infinite chain limit $N\to\infty$. The SSH Hamiltonian has only two independent parameters apart from an overall energy scale. We choose them to be the phonon frequency at wave vector $2k_F=\pi$, $\omega=2\sqrt{D/M}$, and the reduced electron-phonon coupling constant $g=\alpha/\sqrt{Dt}$. Su, Schrieffer, and Heeger have studied the properties of this model, for $n=2$, in the static limit $M\to\infty$. In this limit they showed that the ground state is always dimerized for a half-filled-band system. This result is correct, at $M\to\infty$, for all n since the spin plays very little role in this semiclassical limit. If one assumes that the lattice is perfectly dimerized, so that the displacements are of the form

$$q_j=(-1)^j m_p \tag{2.2}$$

with m_p the phonon (staggered) order parameter, the value of m_p that minimizes the total ground-state energy of the system satisfies the equation

$$1=\frac{8g^2}{\pi}\int_0^{\pi} dk(\sin^2 k)\times[4t^2\cos^2 k+(4g\sqrt{D/t}\,m_p)^2\sin^2 k]^{-1/2} \tag{2.3}$$

in the limit $N\to\infty$. For small values of the coupling constant g one finds

$$gm_p\cong\frac{2}{e}\sqrt{t/D}\,e^{-\pi/2ng^2}\,. \tag{2.4}$$

One can also define an electron order parameter for this model given by

$$m_e=\frac{1}{N}\sum_{j=1}^{N}\sum_{s=1}^{n}(-1)^j\langle 0\,|\,C_{j,s}^{\dagger}C_{j+1,s}+\text{H.c.}\,|\,0\rangle\,, \tag{2.5}$$

where $|\,0\rangle$ is the ground state of the system. This order parameter measures the difference in the electronic density of the short and long bonds in the chain. In the $M\to\infty$ limit it is related to the phonon order parameter by

$$m_e=\frac{2}{g}\sqrt{D/t}\,m_p\,. \tag{2.6}$$

As a matter of fact, Eq. (2.6) is just the condition for mean-field theory of the Hamiltonian (2.1) to be self-consistent.

Finally, the gap in the electronic spectrum is related to the staggered phonon displacment by $\Delta=4\alpha m_p$ and has the asymptotic form

$$\Delta\cong\frac{8t}{e}e^{-\pi/2ng^2}\,. \tag{2.7}$$

Equations (2.7) and (2.4) predict the existence of long-range dimerization order and a gap in the electronic spectrum for the arbitrarily small coupling constant g and arbitrary electronic spin n. We will study now how this result is affected when the phonons have a finite frequency ($M<\infty$) so that they can undergo zero-point quantum fluctuations.

We start by constructing a continuum field theory, which describes the long-distance behavior of this model. For the case $n=2$, Takayama, Lin-Liu, and Maki[3] (TLM) have constructed a continuum theory and studies its adiabatic limit. With some minor modifications the continuum theory we propose is that of TLM. However, we will discuss fluctuation effects quite explicitly.

The continuum theory has a Hamiltonian density given by

$$H=\sum_{s=1}^{n}\int dx\,\psi_s^{\dagger}(x)\left[-i\frac{\partial}{\partial x}\right]\sigma_3\psi_s(x)+\int dx\left[\frac{1}{2}\left[\frac{\partial\phi}{\partial x}\right]^2+\frac{1}{2M}\pi^2(x)\right]+\int\left[\frac{1}{8Ma_0^2}\Gamma(x)^2+\tfrac{1}{2}\Delta(x)^2\right]dx$$
$$+\sqrt{2g}\int dx\,\Delta(x)\sum_{s=1}^{n}\bar{\psi}_s(x)\psi_s(x)+\frac{iga_0}{2}\int dx\,\phi(x)\sum_{s=1}^{n}\left[\psi_s^{\dagger}(x)\frac{\partial^2}{\partial x^2}\sigma_3\psi_s(x)-\frac{\partial^2\psi_s^{\dagger}}{\partial x^2}(x)\sigma_3\psi_s(x)\right], \tag{2.8}$$

where we have set $D=1$. This formula requires some explanation. First, $\psi(x)$ is a doublet (a spinor) made up of the right-moving $\psi_{1s}(x)$ and left-moving $\psi_{2s}(x)$ components of the Fermi field near the Fermi points. The two scalar fields $\phi(x)$ and $\Delta(x)$, represent the acoustic ($k\to 0$) and dimerization ($k\to\pi$) pieces of the phonon spectrum respectively. The canonically conjugate momenta are $\pi(x)$ and $\Gamma(x)$, respectively:

$$[\phi(x),\pi(y)]=i\delta(x-y)\,,$$
$$[\Delta(x),\Gamma(y)]=i\delta(x-y)\,. \tag{2.9}$$

In Eq. (2.8) Feymann's $\bar{\psi}$ notation is used. The Dirac γ matrices in two dimensions are chosen to be

$$\gamma_0=\sigma_2=\begin{bmatrix}0 & -i\\ i & 0\end{bmatrix}$$
$$\gamma_5=\sigma_3=\begin{bmatrix}1 & 0\\ 0 & -1\end{bmatrix}=\alpha\ ,$$
$$\gamma_1=\gamma_0\alpha=i\sigma_1=\begin{bmatrix}0 & i\\ i & 0\end{bmatrix}\ , \tag{2.10}$$
$$\bar{\psi}_s=\psi_s^\dagger\gamma_0\ .$$

Thus the electron dimerization order parameter is

$$m_e=\sum_{s=1}^{n}\langle 0\,|\,\bar{\psi}_s(x)\psi_x(x)\,|\,0\rangle$$
$$=i\sum_{s=1}^{n}\langle 0\,|\,[\psi_{2s}^\dagger(x)\psi_{1s}(x)$$
$$-\psi_{12}^\dagger(x)\psi_{2s}(x)]\,|\,0\rangle \tag{2.11}$$

and the ground state is dimerized whenever $m_e\neq 0$. Note that $\mathscr{H}$ has a discrete global symmetry

$$\psi_s\to\psi_s'=\gamma_5\psi_s\ ,\quad \bar{\psi}_s\to\bar{\psi}_s'=-\bar{\psi}_s\gamma_5,$$
$$\Delta(x)\to-\Delta(x)\ . \tag{2.12}$$

The dimerized state breaks this symmetry, since

$$\sum_{s=1}^{n}\bar{\psi}_s(x)\psi_s(x)\to-\sum_{s=1}^{n}\bar{\psi}_s(x)\psi_s(x) \tag{2.13}$$

under this symmetry.

A few words about dimensions are needed. In formula (2.8) we have set the Fermi velocity equal to one. Thus space and time are measured in units of length L. Likewise, the Fermi fields $\psi_s(x)$ have units of $L^{-1/2}$, the acoustic-phonon field ϕ is dimensionless, and the dimerization field $\Delta(x)$ has units of L^{-1}. This choice of dimensions explicitly renders the coupling constant between the fermions and the field $\Delta(x)$ dimensionless.

Before we begin a study of the properties of this Hamiltonian a few comments are in order. Equation (2.8) contains all the leading and next-to-leading terms in a power-series expansion in a_0, the lattice spacing. Such a naive approach is justified in the case of polyacetylene since SSH (Ref. 1) have shown that the width of the soliton is of the order of seven lattice constants, and hence a continuum approach is well founded. However, in general we must take care that all relevant terms, in the renormalization-group sense, are kept. Otherwise some important physics will be missing. We argue that Eq. (2.8) contains all the possible relevant and marginal operators that can arise from the SSH model. Since the coupling constant g is dimensionless, ga_0 has dimensions of length. Therefore, the operator

$$\phi(x)\psi_s^\dagger\sigma_3(\partial^2/\partial x^2)\psi_s$$

is expected to be irrelevant by power counting. Higher-order terms in a_0 will bring only higher irrelevant operators that cannot change the physics of the ground state and the low-lying spectrum. Of course, irrelevant operators do contribute to fermionic excitations away from the Fermi surface. The Hamiltonian (2.8) can be in fact further simplified by dropping the last term. The acoustic part of the phonon spectrum thus decouples from the physics of the low-energy spectrum and may be ignored altogether. It should be stressed that the continuum model (2.8) is a model for the low-energy part of the spectrum of the SSH model. The fields included in (2.8) are slowly varying on the scale of the lattice spacing. However, Eq. (2.8) is also an ultralocal approximation to the lattice theory. In the derivation, which we do not give here, nonlocal, cutoff-dependent terms arise and we have not included them here, in the spirit of a continuum theory. However, their very existence implies that wherever we multiply continuum operators at the same point, a point-splitting prescription should be assumed. The importance of this remark will become apparent in the next section.

A. The spinless case ($n=1$)

As was stated above, we want to understand the role of both spin fluctuations as well as quantum fluctuations of the phonon field. We then begin our discussion by considering the case of spinless electrons. This case may seem superficially unphysical since electrons always carry spin. However, in the presence of a magnetic field H spin fluctuations are suppressed and the low-energy Hamiltonian is given by Eq. (2.8) with $n=1$. In other words a term of the form

$$\int d^3x\, H\psi_1^\dagger(x)\psi_1(x) \tag{2.14}$$

will appear in the Hamiltonian and the spin symmetry [SU(n)] will be explicitly broken. This term is relevant in the renormalization-group sense. As mentioned earlier, another instance of spinless electrons is found by means of a Jordan-Wigner transformation of the SSH Hamiltonian with $n=1$, which yields the spin-Peierls problem for the XY spin chain. The results of SSH at large M have been reviewed at the beginning of this section. Let us consider the opposite limit: $M\to 0$.

1. The zero mass limit

In the $M \to 0$ limit the deformation field $\Delta(x)$ can be integrated out explicitly. The Lagrangian in this limit is

$$\mathscr{L} = i\bar{\psi}\partial\psi - \frac{\Delta^2}{2} - \sqrt{2}g\Delta\bar{\psi}\psi \ . \tag{2.15}$$

After the bosons are integrated out an effective fermion Lagrangian is found,

$$\mathscr{L} = i\bar{\psi}\partial\psi + g^2(\bar{\psi}\psi)^2 \ . \tag{2.16}$$

This is the Lagrangian density of the $n=1$ Gross-Neveu model.[8] As a matter of fact that argument works for arbitrary n yielding an effective Lagrangian

$$\mathscr{L} = i\sum_{s=1}^{n}\bar{\psi}_s\partial\psi_s + g^2\left[\sum_{s=1}^{n}\bar{\psi}_s\psi_s\right]^2 , \tag{2.17}$$

which is the SU(n) Gross-Neveu model.[8]

Returning to Eq. (2.16) we can use the formula, valid only for $n=1$ (Ref. 11),

$$(\bar{\psi}\psi)^2 = \delta(0)\psi^\dagger\psi - \tfrac{1}{2}(\bar{\psi}\gamma_\mu\psi)^2 - [(\psi_1^\dagger\psi_2)^2 + (\psi_2^\dagger\psi_1)^2] \tag{2.18}$$

to write the effective Lagrangian in the form of the massless Thirring (or Luttinger) model

$$\mathscr{L} = i\bar{\psi}\partial\psi - \frac{g^2}{2}(\bar{\psi}\gamma_\mu\psi)^2 - [(\psi_1^\dagger\psi_2)^2 + (\psi_2^\dagger\psi_1)^2] + \delta(0)\psi^\dagger\psi \ . \tag{2.19}$$

The first two terms form the Lagrangian density of the massless Thirring model. The fourth term is an (infinite) chemical potential and may be ignored. The third term $(\psi_2^\dagger\psi_1)^2 + (\psi_1^\dagger\psi_2)^2$ apparently vanishes because of Fermi statistics. However, this is a dangerous argument since we are multiplying quantum fields at the same point and quantum fluctuation may yield a nonvanishing contribution. Indeed this is the case as was discussed in great detail by den Nijs.[12]

As a matter of fact, the Lagrangians (2.16) and (2.19) have different symmetries if the third term is dropped. The massless Thirring model is invariant under the global continuous [U(1)] chiral transformation

$$\psi \to \psi' = \exp(i\gamma_5\theta), \quad 0 \le \theta < 2\pi$$
$$\bar{\psi} \to \bar{\psi}' = \bar{\psi}\exp(+i\gamma_5\theta) \ , \tag{2.20}$$

while (2.16), the $n=1$ Gross-Neveu model, has only a discrete chiral symmetry

$$\psi \to \psi' = i\gamma_5\psi, \quad \bar{\psi} \to \bar{\psi}' = i\bar{\psi}\gamma_5 \ . \tag{2.21}$$

The third term in (2.19) breaks the continuous chiral symmetry (2.20) down to the discrete symmetry (2.21). Since this chiral symmetry is discrete, it can be spontaneously broken leading to a phase in which $\langle\bar{\psi}\psi\rangle \neq 0$ and the system is dimerized. The continuous symmetry (2.20) cannot be spontaneously broken in one dimension ($T>0$) due to the Mermin-Wagner theorem.[13]

The phase transition to a dimerized state occurs only if g is strong enough. This result can also be obtained in the $M=0$ case for the lattice version of the SSH model, Eq. (2.1). By writing the phonon part as a functional integral and integrating out the phonon degrees of freedom, we obtain the exact effective Hamiltonian

$$H = -t\sum_j (C_j^\dagger C_{j+1} + \text{H.c.}) - \frac{g^2}{2}\sum_j (C_j^\dagger C_{j+1} + \text{H.c.})^2 \ ,$$

which, using the commutation relations, can be rewritten as

$$H = -t\sum_j (C_j^\dagger C_{j+1} + \text{H.c.}) + g^2\sum_j n_j n_{j+1} - g^2\sum_j n_j \ . \tag{2.22}$$

Thus the fermions experience an effective *repulsive* force between nearest neighbors. For $g^2/2t = 1$ the system undergoes a transition to a charge-density-wave state. This can also be visualized by noting that the Hamiltonian equation (2.22) is, via a Jordan-Wigner transformation, equivalent to the *XXZ* antiferromagnetic spin chain. The phase transition takes place at the isotropic point.

We follow Witten[14] and den Nijs[12] in analyzing the model at $M=0$ by introducing the boson representation of the fermion fields. The equivalent Bose field[15–19] $\eta(x)$ has a Lagrangian density equal to

$$\mathscr{L} = \tfrac{1}{2}(\partial_\mu\eta)^2 + \frac{g^2\Lambda^2}{\pi^2}\cos[2\beta\eta(x)] \ , \tag{2.23}$$

where

$$\beta^2 = (16\pi)\left[1 + \frac{2g^2}{\pi}\right]^{-1} .$$

The last term in (2.18) originates from the short-distance expansion of $(\psi_1^\dagger\psi_2)^2 + (\psi_2^\dagger\psi_1)^2$ in the boson representation. The coefficient of $\cos(2\beta\eta)$,

$$z = \frac{\alpha}{\beta^2} = \frac{g^2}{\pi^2} \ , \tag{2.24}$$

which plays the role of a coupling constant (or "fugacity"), is defined in terms of a large momentum cutoff Λ *in the boson theory.* However, as den Nijs[12] has discussed quite extensively, there is a critical value of $g=g_c$ (where $\beta_c^2=8\pi$) below which the $\cos(2\beta\eta)$ operator is *relevant* and cannot be ignored.

The renormalization-group properties of (2.23) are well known.[19–22] The long-distance behavior of (2.23) is controlled by the Kosterlitz renormalization group (see Fig. 1). The model (2.23) lives on the physical curve

$$y=\tfrac{1}{2}(2-x)\,, \tag{2.25}$$

where $y=\frac{1}{4}\alpha$ and $x=2(\beta^2/8\pi-1)$, following Amit *et al.*[21] As indicated in the figure there is an intersection between this curve and the separatrix $y=x$. They meet at $g_c^2=\pi/4$.

It is important to stress that the Lagrangian (2.22) contains all the relevant and marginal operators that can be generated from the short-distance expansion of the SSH model at $M=0$ for $g^2\lesssim\pi/4$. Of course, the actual SSH Hamiltonian contains a large (infinite) number of irrelevant operators. But these operators give negligible contribution for $g\lesssim\pi/4$ since their coupling constants include powers of the lattice constant.

The discussion sketched above follows the work of den Nijs[12] very closely. The point of reproducing it here is to clarify the role of some symmetries and the effect of retardation.

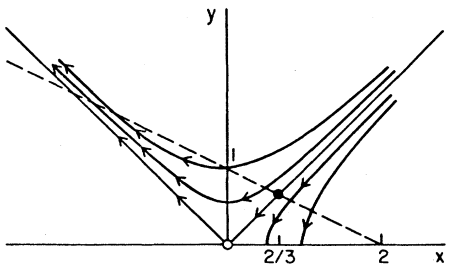

FIG. 1. Renormalization-group flow of Kosterlitz (schematic). The dashed line represents the initial values of x and y accessible for the $n=1$ SSH model. The dot is the phase transition point.

2. *Finite mass*

At finite ionic mass M the phonons can still be integrated out, however, at the price of introducing retardation effects. For finite mass the Lagrangian, after dropping the acoustic phonons, is

$$\mathcal{L}=i\bar{\psi}\partial\psi+\tfrac{1}{2}m\dot{\Delta}^2-\frac{\Delta^2}{2}-\sqrt{2}g\Delta\bar{\psi}\psi\,, \tag{2.26}$$

where $m=4(Ma_0^2)\equiv 1/\omega^2$.

The Bose field Δ can be integrated out explicitly yielding an effective action s_{eff} for the Fermi fields

$$\exp(iS_{\text{eff}}[\bar{\psi},\psi])=\int D\Delta\exp\left[i\int dx\,dt\,\mathcal{L}\right], \tag{2.27}$$

with

$$S_{\text{eff}}=\int dx\,dt\,i\bar{\psi}\partial\psi+g^2\int dx\int dt\int dt'\bar{\psi}(x,t)\psi(x,t)G(t-t')\bar{\psi}(x,t')\psi(x,t)\,. \tag{2.28}$$

The Green's function $G(t-t')$ is equal to

$$G(t-t')=i\langle 0\,|\,T[\,\Delta(x,t)\Delta(x,t')]\,|\,0\rangle=\frac{\omega}{2}\exp(-i\,|\,t-t'\,|\,\omega)\,. \tag{2.29}$$

Hence the effective action is nonlocal in time. However, we are only interested in the low-energy behavior (i.e., ground-state and low-lying excitations) of the system. In this limit the fields $\psi(x,t)$ are slowly varying both in space and time. Thus if we study states with an excitation energy $\Delta E\ll\omega$, the nonlocal effects should be unimportant for them. Quite to the contrary, there will be states with excitation energies of the order ω for which retardation effects are essential. Since ω is proportional to $1/\sqrt{M}$ we see that as the ions get lighter most of the actual spectrum lies in the region $\Delta E\ll\omega$. But in the classical limit ($M\to\infty$) the region of validity of our approximations shrinks to zero. We are going to argue in the next section that as $M\to\infty$ the semiclassical treatment should be exact.

Let us define an operator $J(x,t)\equiv\bar{\psi}(x,t)\psi(x,t)$. Then the effective action reads

$$\begin{aligned}S_{\text{eff}}&=\int dx\,dt\,i\bar{\psi}\partial\psi+g^2\int dx\int dt\,dt'J(x,t)G(t-t')J(x,t')\\&=\int_{-\infty}^{+\infty}dx\int dt\,i\bar{\psi}\partial\psi+\frac{g^2}{2}\int_{-\infty}^{+\infty}dx\int_{-\infty}^{+\infty}dt\int_0^{\infty}ds\,\omega J(x,t)[J(x,t+s)+J(x,t-s)]e^{-\omega s}\,.\end{aligned} \tag{2.30}$$

By expanding $J(x,t\pm s)$ in powers of s we find an effective Lagrangian

$$\mathscr{L}_{\text{eff}}=i\,\bar{\psi}\partial\psi+g^2\sum_{n=0}^{\infty}\left[\frac{\partial^n}{\partial t^n}J(x,t)\right]^2\frac{1}{\omega^{2n}}\ . \tag{2.31}$$

We can rewrite the effective Lagrangian to read

$$\mathscr{L}_{\text{eff}}=i\,\bar{\psi}\partial\psi+g^2(\bar{\psi}\psi)^2+\frac{g^2}{\omega^2}\left[\frac{\partial}{\partial t}\bar{\psi}\psi\right]^2+\cdots\ . \tag{2.32}$$

Thus the effect of finite mass, and hence all retardation effects, are terms of the form

$$\left[\frac{\partial^{(n)}}{\partial t^{(n)}}\bar{\psi}\psi\right]^2 .$$

In the boson representation, these terms will render operators of the form

$$\left[\frac{\partial^{(n)}}{\partial t^{(n)}}\partial_\mu\eta\right]^2 \text{ and } \left[\frac{\partial^{(n)}}{\partial t^{(n)}}\cos\beta\eta\right]^2 ,$$

etc. All these terms contain explicit derivatives and thus have dimensions higher than those in (2.22). Those operators are irrelevant by power counting and remain irrelevant for $g^2\lesssim\pi/4$, dropping out from the physics at low energies. We then conclude that the properties of the system near (and below) the dimerization transition are independent of the mass of the ions and, so far as M is *finite* they are always controlled by the behavior at $M=0$. In some sense ω, the excitation energy of the Bose field, plays the role of an energy-scale intermediate between the low-energy (scaling) regime and the cutoff (bandwidth) scale. If the system is probed at different energies a crossover should be observed between the Gross-Neveu behavior ($\Delta E\ll\omega$) and the semiclassical behavior ($\Delta E\gg\omega$). The crossover region will not be present in the semiclassical limit ($M\to\infty$) in which it is a nonperturbative effect. Thus the calculations of SSH (Refs. 1 and 2) should be accurate for states with excitation energies much bigger than ω, while our considerations apply to the low-energy part of the spectrum only.

The massless Thirring model, and for these matters the same applies to the Gross-Neveu models, relate to the fermion-boson Lagrangian (2.26) in another interesting way. The Lagrangian (2.26) represents a coupling between relativistic fermions ψ and nonpropagating bosons Δ. "Elastic" terms, i.e., $(\partial\phi/\partial x)^2$, are of course going to be generated in perturbation theory. In some sense the dimension that we have assigned to the boson field Δ is not the standard dimension for a Bose field. Our assignment is completely natural at $M=0$ but not so natural when $M\neq0$ and "elastic" terms are present. In such situations one may expect Δ to be dimensionless in one dimension. The coupling constant g would not then be dimensionless in one dimension, but rather, in three. Something very similar happens in ϕ^4 field theory in its relation to the nonlinear σ model. Indeed, the Gross-Neveu models have properties very much analogous to the nonlinear σ models, while (2.26) is naturally closer to ϕ^4 theory. The standard procedure of writing down an effective Lagrangian for the Goldstone modes of ϕ^4 theory, which yields the nonlinear σ models, parallels the line of arguments that we used to eliminate the retardation effects.

3. *Phase diagram*

We can now collect the results of Secs. II A 1 and II A 2 together with the results of SSH (Refs. 1 and 2) and TLM (Ref. 3) for $M\to\infty$ into a phase diagram (Fig. 2). The half-filled-band spinless SSH model has two phases.

(i) The first is a strong coupling phase in which the ground state is dimerized. The system, on a lattice, is invariant under translations by two lattice spacings (Peierls instability). In the continuum model the discrete chiral symmetry $\psi\to i\gamma_5\psi$ is broken and the dimerization order parameter $\langle\bar{\psi}\psi\rangle$ has a nonvanishing expectation value. The fermion spectrum has a gap. In Sec. II A 1 we showed that this was indeed the case for $M=0$ if $g^2>g_c^2\simeq\pi/4$. In Sec. II A 2 we showed that these results extend to finite M provided that the system is close enough to criticality, where the continuum limit results are valid. On the other hand both SSH (Refs. 1 and 2) and TLM (Ref. 3) have shown that the system al-

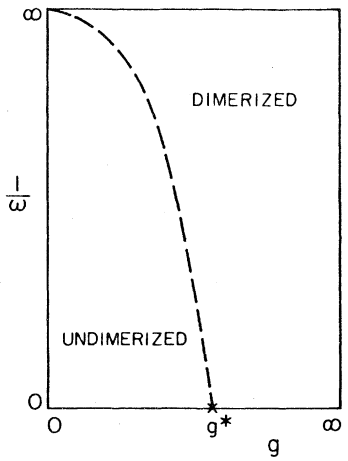

FIG. 2. Qualitative phase diagram for the $n=1$ SSH model.

ways dimerizes as $M \to \infty$ for all g.

(ii) The second is a weak coupling phase in which the ground state is not dimerized and $\langle \bar{\psi}\psi \rangle = 0$. This phase is, as a matter of fact, critical since the Green's functions are long ranged. No soliton states are present in this case (they are actually massless). The critical phase is expected to exist up to arbitrarily large ionic masses so far as g is small enough. For very large M the arguments given in Sec. II A 2 about the irrelevance of the extra operators fail since $\omega \to 0$ and the effective Lagrangian becomes truly nonlocal.

(iii) The model also has a phase boundary, which is depicted in the figure. This transition is of the Kosterlitz-Thouless type. Close enough to this line the SSH model ($n=1$) behaves like the boson Lagrangian (2.32).

B. The spin-$\frac{1}{2}$ SSH model ($n=2$)

This is the case of actual interest for a polyacetylene chain without a magnetic field. The physics for $n>1$ (all n) is actually very similar to the case of $n=2$ except for some special properties of the spectrum at $n=2$.

The formalism used to describe the $n=1$ model in Sec. II A applies for general n. The physics of the models with $n>1$ is, however, very different. Once again we will write down a continuum model that represents the system near the dimerization phase transition.

1. The zero mass limit ($M \to 0$)

We begin our discussion by considering the SSH continuum model in the limit where the mass of ions vanishes. The Lagrangian density, after integrating out the bosons, is

$$\mathcal{L} = i \sum_{s=1}^{n} \psi_s \partial \psi_s + g^2 \left[\sum_{s=1}^{n} \bar{\psi}_s \psi_s \right]^2 . \tag{2.33}$$

It was pointed out in Sec. II A 1 that this is the Lagrangian of the Gross-Neveu (GN) model. This model has been extensively studied and even though it has not been solved exactly so far, many of its properties are by now well understood.

Let us first summarize the properties of this model. It has the following symmetries:

(i) A continuous SU(n) symmetry $\psi' = U\psi$ where U is an SU(n) matrix. This is just the spin rotation symmetry of the SSH model. This symmetry remains unbroken.

(ii) A discrete chiral symmetry $\psi' = i\gamma_5 \psi$, already present in the $n=1$ model. This symmetry turns out to be broken for *all* values of the coupling constant g. The order parameter $\langle \bar{\psi}\psi \rangle$ is thus nonvanishing for all $g \neq 0$.

Gross and Neveu studied both the renormalization-group properties of this model as well as its behavior in the semiclassical limit $n \to \infty$. In the critical phenomena language they found that the β function for the dimensionless coupling constant g has only one infrared unstable fixed point, at $g^* = 0$, and that the theory is asymptotically free. That is to say, the effective coupling constant at short distances is small while at long distances it is large; the system always iterates to strong coupling in the infrared. Specifically, to one-loop order they found

$$\beta(g) = \frac{\partial g}{\partial \ln a_0} = \left[\frac{n-1}{\pi} \right] g^3 , \tag{2.34}$$

where g^2 is the (bare) dimensionless coupling constant and a_0 is the lattice spacing. This result clearly shows that g becomes relevant due to fluctuation effects.

Gross and Neveu further studied this model and considered the large-n limit. In this limit, where the Hartree approximation is exact, they found that the operator $\bar{\psi}\psi$ acquires a nonvanishing expectation value for all $g>0$. The system is dimerized and the discrete chiral symmetry is broken. There is a gap in the single-particle spectrum equal to Δ_F,

$$\Delta_F = \Lambda \exp\{-\pi/\bar{g}^2\} , \tag{2.35}$$

as $n \to \infty$. In (2.35) $\bar{g}^2 = ng^2$ and $\Lambda \sim 1/a_0$. The order parameter $\langle \bar{\psi}\psi \rangle$ is equal to Δ_F/g^2. The physics of the GN model in large n is thus very similar to the $M \to \infty$ limit of SSH and TLM.

The GN model has been further studied, in the semiclassical (i.e., large-n) limit, by Dashen, Hasslacher, and Neveu[23] (DHN), who found an enormously rich spectrum of solitons, solitons-antisolitons bound states, etc. The results of DHN for large n, as well as some of their conjectures for finite n, have been confirmed by an exact calculation of the S matrix of the GN model by Zamolodchikov and Zamolodchikov,[24] Witten,[14] and, more recently, by Karowski and Thun.[25] Of particular interest for the physics of polyacetylene is the finding that the soliton-antisoliton ($s\bar{s}$) bound state becomes unstable at $n=2$ (Ref. 24). Indeed, these studies find that the energy of an $s\bar{s}$ bound state is equal to[22,23]

$$E^j_{s\bar{s}} = 2E_{\text{kink}} \sin[\pi j/2(n-1)] ,$$
$$j = 1, \ldots, <n-1 . \tag{2.36}$$

Thus for $n=2$ we have $E_{s\bar{s}} = 2E_{\text{kink}}$ and the binding energy vanishes. This result implies that the binding energy of a polaron, a bound state of soliton, antisoliton, and a fermion, must also vanish as $n \to 2$. Thus polaron states must be unstable for the SSH

model in the continuum limit. Even though this result is actually true for $M=0$ we are going to argue shortly that it ought to hold wherever the continuum model applies. In contrast, the polaron state is known to be stable in the $M=\infty$ limit for $n=2$. We will return to this point at the end of this section.

2. Finite mass

We use a renormalization-group treatment to analyze the role of a finite ionic mass M, and hence retardation effects. A line of thought similar to the arguments that led to the effective Lagrangian (2.32) in the spinless case yields the natural generalization

$$\mathscr{L}_{\text{eff}}=\sum_{s=1}^{n} i\bar{\psi}_s\partial\psi_s+g^2\left[\sum_{s=1}^{n}\bar{\psi}_s\psi_s\right]^2 +\frac{g^2}{\omega^2}\left[\sum_s\frac{\partial}{\partial_t}\bar{\psi}_s\psi_s\right]^2+\cdots . \tag{2.37}$$

The continuum Fermi fields ψ_s have dimensions of (length)$^{-1/2}$. This implies that the coupling constant g is dimensionless but, also, that the coupling constant for $(\sum_s \partial/\partial t\bar{\psi}_s\psi_s)^2$ must have dimensions of (length)^2. Hence $(\sum_s \partial/\partial t\bar{\psi}_s\psi_s)^2$ is superficially an irrelevant operator of two dimensions. The higher-order terms [i.e., $O(1/\omega^4)$ and higher] have even larger dimension and hence are more irrelevant. This naive power counting argument is correct because the infrared unstable fixed point at $g=0$, where the transition to the dimerized state takes place, is asymptotically free. In such situations fluctuation effects will only produce small logarithmic corrections to free-field results.

These claims can be readily verified by modifying the renormalization-group treatment of Gross and Neveu[8] in the presence of a finite mass M. Let $\Gamma_B(x,y)$ be the inverse propagator for the Bose field $\Delta(x)$, i.e.,

$$\Gamma_B^{-1}(x,y)=\langle 0\,|\,T[\Delta(x)\Delta(y)]\,|\,0\rangle , \tag{2.38}$$

where $x\equiv(x,t)$ and $y\equiv(y,t')$ and $|0\rangle$ is the exact ground state.

The unperturbed boson propagator, in momentum-frequency space, is

$$\Gamma_B(p,\omega)=-i(-M\omega^2+1-i\epsilon) , \tag{2.39}$$

which reflects the nonpropagating nature of the (decoupled) field Δ. However, since fermion-boson interactions will generate propagating terms we are forced to write a more general form for the bare propagator,

$$\Gamma_B(p,\omega)=-i(1-M\omega^2+sp^2-i\epsilon) . \tag{2.40}$$

The parameter s is equal to zero at the starting point. Dimensionally, M and s are very similar; they both have dimensions of (length)^2. It is more convenient to define the dimensionless parameters $\bar{M}$ and $\bar{s}$,

$$\bar{M}=M\Lambda^2 , \quad \bar{s}=s\Lambda^2 , \tag{2.41}$$

where $\Lambda\sim 1/a_0$, a_0 being a length of the order of the lattice spacing.

A straightforward renormalization-group calculation shows that the parameters $\bar{M}$ and $\bar{s}$ are irrelevant. An explicit calculation, to one-loop order, yields the result

$$\beta_{\bar{M}}=\frac{\partial\bar{M}}{\partial\ln a_0}=-2\bar{M}\left[1+g^2\left[\frac{n-1}{\pi}\right]\right] ,$$
$$\beta_{\bar{s}}=\frac{\partial\bar{s}}{\partial\ln a_0}=-2\bar{s}\left[1+g^2\left[\frac{n-1}{\pi}\right]\right] . \tag{2.42}$$

These β functions, when complemented by the Gross-Neveu β function, Eq. (2.34), show that $\bar{M}$ and $\bar{s}$ not only are irrelevant but also become more irrelevant due to fluctuation effects. Thus there is only one infrared unstable fixed point still located at $g^*=0$.

Equations (2.42) enable us to investigate the role of these irrelevant operators. It is useful to eliminate the implicit dependence in a_0 from (2.42) and (2.34) to investigate the dependence of $\bar{M}$ on the effective coupling constant at a given length scale. By taking the ratio of (2.42) and (2.34) we find

$$\frac{\partial\ln\bar{M}}{\partial g}=\frac{\partial\ln\bar{s}}{\partial g}=-\left[\frac{2\pi}{n-1}\right]\frac{1}{g^3}\left[1+g^2\left[\frac{n-1}{\pi}\right]\right] . \tag{2.43}$$

This equation can be integrated to yield the result

$$\ln\bar{M}-\left[\frac{\pi}{n-1}\right]\frac{1}{g^2}+2\ln g=\text{const} , \tag{2.44}$$

or, equivalently, the result in which $\bar{M}$ has the following dependence on g, the coupling constant at the scale a_0:

$$\bar{M}=\frac{\text{const}}{g^2}\exp\left[+\frac{\pi}{(n-1)g^2}\right] . \tag{2.45}$$

Thus as $a_0\to\infty$, $g\to\infty$ and $\bar{M}\to 0$. Conversely, as $a_0\to 0$, $g\to 0$ and $\bar{M}\to\infty$, thus showing that irrelevant operators, while dropping out from long-distance physics, make an overwhelming effect at short distances. The renormalization-group flow (2.45), (2.34) is shown in Fig. 3. In other words, the coupled electron-phonon system for $n>1$ is in the universality class of the Gross-Neveu model for the

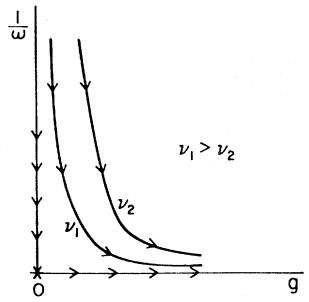

FIG. 3. Qualitative renormalization-group flows for the $n=2$ SSH model. Note that the trajectory with the largest value of ν gets closer to the asymptotic trajectory faster.

same value of n. In any practical situation, however, some amount of this irrelevant operator will always be present. The problem is then to determine how strong the coupling constant g will become for $\overline{M}$ to be reduced by a factor of σ (for example, 10). If the effective coupling constant is less than one then most of the low-lying spectrum will not be affected by the irrelevant operator. This is so since the gap in the fermionic spectrum behaves like[8]

$$\Delta_F \sim \Lambda \exp\left[-\frac{\pi}{2(n-1)g^2}\right] \tag{2.46}$$

(in the GN limit), becoming very small if g is small. However, should g become of the order of unity the gap would be of the order of Λ (the cutoff) and we would have no reason to drop the irrelevant operator. The upshot is that a criterion for estimating the maximum $\overline{M}$ at which retardation effects are unimportant is to set $g<1$. Clearly, the result is a function of the initial coupling as well. Thus for a fixed reduction factor σ, we can set a limit on the initial bare coupling constant to be the solution of the equation

$$\frac{\sigma}{g_0^2} = \exp\left[-\frac{\pi}{n-1}\right]\exp\left[\frac{\pi}{(n-1)g_0^2}\right]. \tag{2.47}$$

Equation (2.47) shows that for a given bare coupling $g<g_0$ retardation effects will drop out from the physics at low energies at a length scale smaller (i.e., a higher energy) than the coherence length $\xi \sim 1/\Delta_F$. Conversely, for $g>g_0$ we will have the opposite situation and retardation effects will be significant for all states except the ground state.

By making use of Eq. (2.47) and the definition of $\omega \sim 1/\sqrt{M}$, we can write Eq. (2.45) in the form

$$\frac{\omega(g)}{g\Delta_F(a,g)} = \text{const} = \nu\ . \tag{2.48}$$

Note that this ratio is dimensionless. Thus if the initial g and M are such that ν is large (i.e., $\omega \gg g\Delta_F$), retardation effects are negligible and the system is always controlled by the Gross-Neveu limit. This *is not* the situation in polyacetylene, where $\nu \sim 0.39$ since $\Delta_F \sim 0.7$ eV, $\omega \sim 0.16$ eV, and $g \sim 0.58$ eV. Therefore, while we expect retardation effects not to affect the nature of the ground state, significant contributions are to be expected to the nature of the low-lying states like solitons, polarons, etc. Since $g \sim 0.58$, polyacetylene is right in the middle of the crossover region between strong and weak coupling. Numerical calculations should be accurate in this regime.

3. *Phase diagram*

Summarizing the results on the SSH model, for a half-filled band and $n>1$, we conclude that it has no structure. The ground state is dimerized throughout the diagram for all M as long as $g \neq 0$. The order parameter $\langle \bar{\psi}\psi \rangle$, which measures the difference in energy between two nearby bonds, is nonvanishing. We have seen that these results apply in both the Gross-Neveu and static limits.

The spectrum of the system, however, changes with both M and n. Low-lying states, like the polaron, while deeply bound in the adiabatic, as well as for large n (all M), become unstable for $n=2$ in the Gross-Neveu limit. Since polyacetylene is in the middle of the crossover region further studies are required to investigate the effects of irrelevant operators on this state.

III. NUMERICAL RESULTS

In this section we present results of Monte Carlo (MC) simulations of the SSH model. The numerical method[6] is based on a direct-space–imaginary-time representation of the phonon and electron fields. The partition function for an N-site ring at temperature $T=1/\beta$ is written as

$$Z = \int \prod_{i,j} dq_{ij} \exp\left\{-\Delta\tau\left[\sum_{i,j}\frac{M}{2}\left[\frac{q_{i+1,j}-q_{i,j}}{\Delta\tau}\right]^2 + \frac{D}{2}(q_{i,j+1}-q_{i,j})^2\right]\right\}$$
$$\times \operatorname{Tr}\prod_{i=1}^{L}\exp\left[\Delta\tau\sum_{j\ \text{even}}[t_{j,j+1}(i)](C_{j,s}^{\dagger}C_{j+1,s}+\text{H.c.})\right]\exp\left[\Delta\tau\sum_{j\ \text{odd}}[t_{j,j+1}(i)](C_{j,s}^{+}C_{j+1,s}+\text{H.c.})\right], \tag{3.1}$$

with

$$t_{j,j+1}(i) \equiv t - \alpha(q_{i,j+1} - q_{i,j}) \ . \tag{3.2}$$

Here, $1 \leq j \leq N$ labels spatial sites and $1 \leq i \leq L$ labels imaginary time. The temperature axis has been divided into L slices of size $\Delta\tau = \beta/L$. The fermion Boltzmann factor has been broken up in such a way that it is now simple to compute the fermion trace by inserting complete sets of intermediate states. Figure 4 shows the resulting two-dimensional lattice for the case $N=4, L=2$. It also shows an example of two possible fermion world lines. Details of this approach are presented in Ref. 6.

In order for the breakup involved in obtaining Eq. (3.1) to be accurate we need to satisfy the conditions

$$\Delta\tau t \ll 1 \ , \tag{3.3a}$$

$$\Delta\tau\omega \ll 1 \ . \tag{3.3b}$$

It should be stressed that our procedure is essentially exact if Eq. (3.3) is satisfied, and no assumption about the relative energy scales of electronic and ionic motions has been made. For practical purposes, it is sometimes useful to use different slicing for electrons and phonons $\Delta\tau_e$ and $\Delta\tau_p$ that satisfy Eqs. (3.3a) and (3.3b), respectively. For large M for example (adiabatic regime), one can take $\Delta\tau_e \ll \Delta\tau_p$ so that the same phonon field occurs in several fermion time slices.

Although we are interested in studying infinite systems at zero temperature, in practice, of course, we can only study finite systems in space and imaginary time. In order to be at sufficiently low temperatures we have to satisfy the further constraints

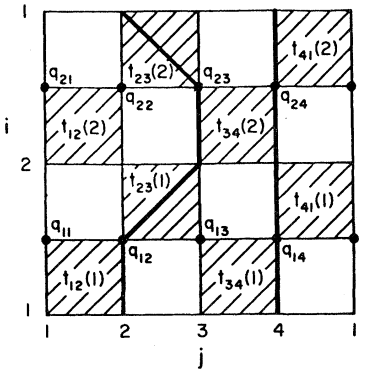

FIG. 4. Space-time lattice for the SSH model and $N=4$, $L=2$. Electrons can only hop across shaded squares, with matrix elements that are a function of the phonon field. The heavy lines are an example of allowed electron world lines.

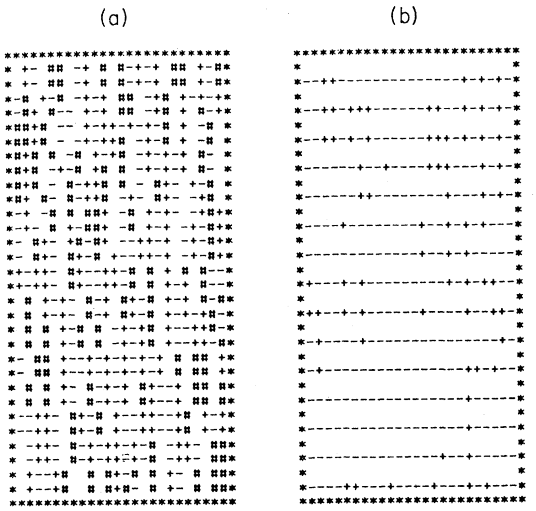

FIG. 5. Typical configuration of the electron and phonon fields for a 24-site ring, and parameters appropriate for polyacetylene: $g=0.58$, $\omega=0.066$, $\Delta\tau_p=10$, $\Delta\tau_e=0.5$, and $\beta=150$. (a) The electron configuration for the first 30 time slices, denoted by + (−) for spin up (down), and # for double occupation. On careful examination a charge-density wave located on the bonds becomes apparent. (b) Sign of the staggered phonon field.

$$\beta t \gg 1 \ , \tag{3.4a}$$

$$\beta\omega \gg 1 \ , \tag{3.4b}$$

and $\beta\Delta \gg 1$, with Δ the gap in the electronic spectrum.

The Monte Carlo procedure consists in going sequentially through the space-time lattice and updating the fermion world lines at each plaquette[6]

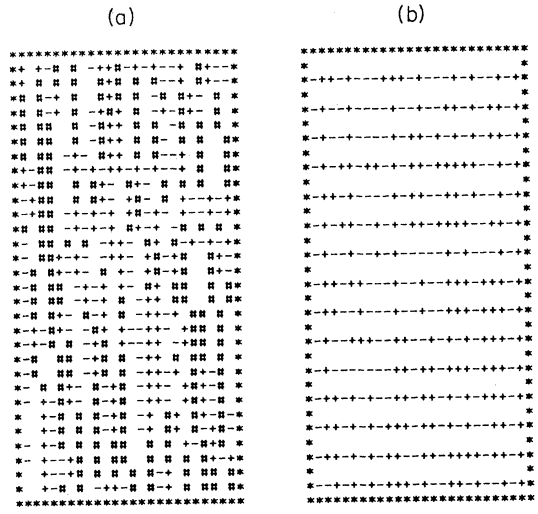

FIG. 6. Same as Fig. 5 with $g=0.58$, $\omega=1$, $\Delta\tau_p=\Delta\tau_e=0.5$, and $\beta=7.5$.

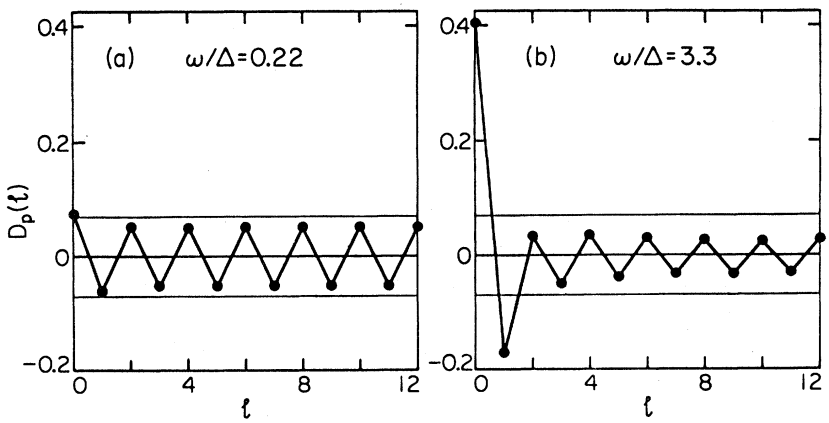

FIG. 7. Phonon spatial correlation function $D_p(l)$. The thin horizontal lines go through the values of $D_p(l)$ in the static limit ($\omega=0$). (a) $g=0.58$, $\omega=0.066$; (b) $g=0.58$, $\omega=1$. Note the much larger zero-point on-site fluctuations ($l=0$) for the smaller ion mass.

and the phonon field at each point. For the phonon-field updating a step size was chosen at random between $-r$ and r, and several updating attempts (three to five) of the phonon field at the site were made in order to bring it in equilibrium with its environment. The maximum step size r was chosen such that the acceptance ratio of these moves was about 0.5. We have tested our program by comparing with known results for electron and phonon properties in the uncoupled limit ($\alpha=0$) and for electron properties in the static limit ($M=\infty$) where the phonon-field coordinates were fixed at a dimerized configuration. It was found that taking $\Delta\tau_e t\sim 0.5$, $\Delta\tau_p\omega\sim 0.5$ gave reasonable agreement (within a few percent) with the exact results in these limits.

Since it is difficult to handle negative weights with our MC algorithm, we have modified somewhat the original model Eq. (2.1). The hopping matrix element in Eq. (3.2) was taken to be

$$t_{j,j+1}(i)=\begin{cases} t-\alpha(q_{i,j+1}-q_{i,j}), & \text{if } q_{i,j+1}-q_{i,j}<t/\alpha \quad (3.5a)\\ 0, & \text{if } q_{i,j+1}-q_{i,j}\geq t/\alpha\ . \quad (3.5b)\end{cases}$$

This modification, of course, makes sense from a physical point of view. As the atoms move away from each other the overlap matrix elements go to zero and do not change sign, as implied by Eq. (3.2). Nevertheless, the theoretical treatment of the preceding section used the form Eq. (3.2), and the phonon coordinates were integrated from $-\infty$ to $+\infty$. We do not think the difference between both models is essential (it certainly is not for small α). Still, we will restrict the numerical study to not too large phonon frequencies so that the hopping matrix elements remain nonzero most of the time.

Most of the results presented in this section are of the more realistic case of electrons with spin ($n=2$). At the end of the section we present some results for

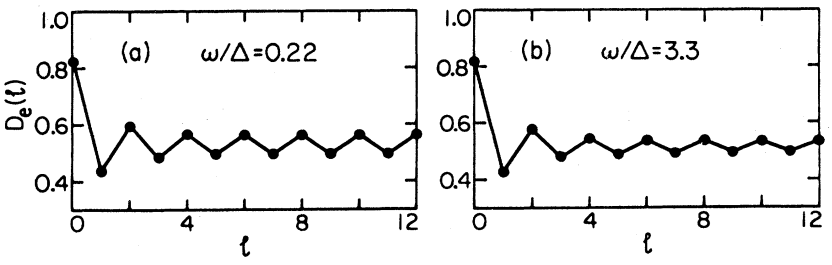

FIG. 8. Electron spatial bond correlation function $D_e(l)$. (a) $g=0.58$, $\omega=0.066$; (b) $g=0.58$, $\omega=1$.

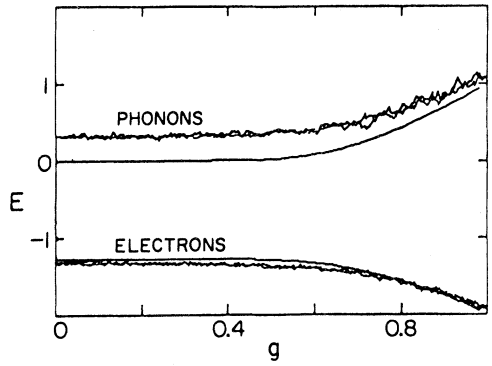

FIG. 9. Energy vs coupling constant for the case $\omega=1$ on a 40×40 lattice, $\Delta\tau_p=\Delta\tau_e=0.5$. Results were obtained from a cycle where g was varied in steps of 0.002 from 0 to 1 and back to 0, and at each point the results of four measurements were averaged. The smooth lines are exact results for the static case ($\omega=0$). Note the appreciable zero-point energy of the phonons (ω/π for $g=0$). The small difference with the static results for the electron energy at $g=0$ is due to the finite $\Delta\tau_e$ used.

the spinless case ($n=1$).

According to SSH,[1] parameters appropriate for polyacetylene are $t=2.5$ eV, $D=21$ eV/Å^2, $\alpha=4.2$ eV/Å, and $M=3145$ eV/Å^2. These give an energy gap of $2\Delta=1.47$ eV, $\omega=0.163$ eV. We have rescaled the units of length and energy so that our rescaled parameters are $t=1$, $D=1$, $\alpha=g=0.58$, and

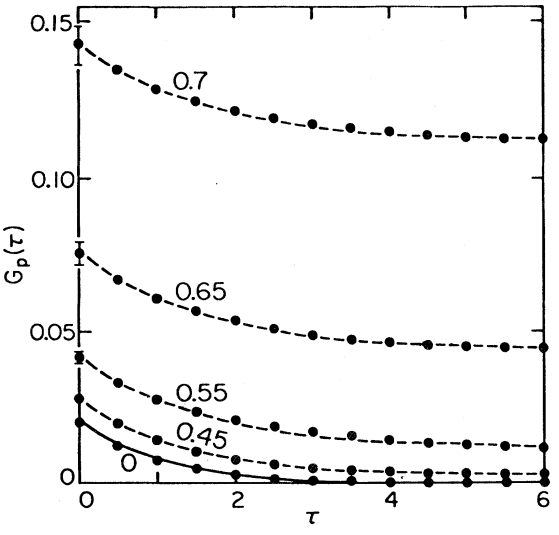

FIG. 10. Phonon order-parameter time correlation function $G_p(\tau)$ for the case $\omega=1$ and several values of g, on a 24×24 lattice, $\Delta\tau_p=\Delta\tau_e=0.5$. The full line is exact results for $g=0$, the dashed lines are fits to the form equation (3.12).

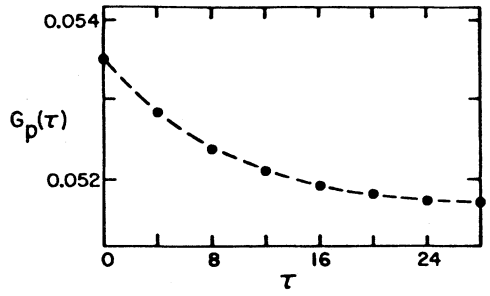

FIG. 11. Phonon order-parameter time correlation function $G_p(\tau)$ for the case of polyacetylene. The dashed line is a fit to the form equation (3.21), which yields $\bar{\omega}/\omega=0.64$.

$M=928$, i.e., $\Delta=0.295$, $\omega=0.666$. For the MC simulation for this case we have taken $\Delta\tau_p=10$, $\Delta\tau_e=0.5$, and $\beta=150$, i.e., 15 phonon time slices and 300 electron time slices, so that conditions (3.3) and (3.4) are approximately satisfied. One needs a very large lattice in the time direction because of the large difference in scale between the electronic and ionic energies.

Figure 5 shows a typical configuration in a MC run for a 24-site ring. In Fig. 5(a) we are plotting only the first 30 fermion time slices. In Fig. 5(b) we are plotting the *staggered* phonon field with a + or − depending on its sign. (There is no correspondence between the fermion and phonon fields shown in Fig. 5, since all fermion time slices shown correspond only to the first two phonon slices.) Note the relatively frequent tunneling of the staggered phonon field to the opposite phase. This has also been previously observed by Su.[26] In the fermion field it is difficult to see the order, since the electron charge-density wave resides on the bonds. Nevertheless, on careful examination it becomes apparent that fermion world lines go diagonally, predominantly between sites $2j$ and $2j+1$, which correspond to short bonds.

Figure 6 shows a typical configuration for the same coupling constant but much smaller mass ($\omega=1$). Here, we have taken $\Delta\tau_e=\Delta\tau_p=0.5$, $\beta=7.5$. Note the larger fluctuations that appear now in the phonon field. Nevertheless, on computing appropriate averages one finds that the system has appreciable long-range order for these parameters too.

Figure 7 shows the phonon spatial correlation functions

$$D_p(l)=\frac{1}{N}\sum_{j=1}^{N}\langle(q_{j+1}-q_j)(q_{j+1+l}-q_{j+l})\rangle \tag{3.6}$$

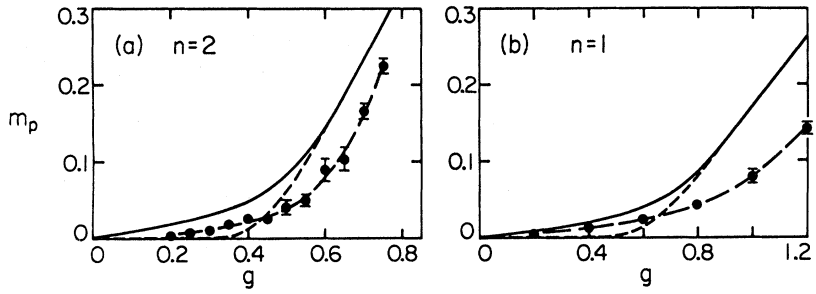

FIG. 12. Phonon order parameter vs g for the case $\omega=1$ on a 24×24 lattice. The full and dashed lines are exact results for the static case on a 24-site lattice and on an infinite lattice, respectively. (a) Spin-$\frac{1}{2}$ case ($n=2$). (b) Spinless case ($n=1$).

for these two cases ($\omega/\Delta=0.22$ and $\omega/\Delta=3.3$ with Δ the classical gap.) These functions show the oscillating behavior characteristic of the dimerized state. For large l one can obtain from it the phonon order parameter m_p, defined as

$$m_p=\frac{1}{2N}\left\langle \sum_{j=1}^{N}(-1)^j(q_{j+1}-q_j)\right\rangle , \tag{3.7}$$

since $D_p(l)\to 4m_p^2$ for large l. For the $(CH)_x$ case there is approximately a 15% reduction in the value of the order parameter from the $\omega=0$ case due to quantum fluctuations. Therefore, the bare interaction for $(CH)_x$ would have to be taken somewhat larger to obtain the gap that is observed experimentally. For $\omega=1$ we should be well into the Gross-Neveu regime, since the parameter ν defined in Eq. (2.48) is about 6. Note how the on-site phonon correlation function grows as ω increases, due to the zero-point fluctuations. At long distances the quantum fluctuations reduce the value of the correlation functions as ω increases. Still, even for a frequency larger than the adiabatic gap ($\omega/\Delta=3.3$) the long-range order is about 60% of the $\omega=0$ value.

Figure 8 shows the corresponding correlation functions for the electrons, defined by

$$D_e(l)=\frac{1}{Nn}\left\langle \sum_{j=1}^{N}\sum_{s}(C_{j,s}^{\dagger}C_{j+1,s}+\text{H.c.}) \times(C_{j+l,s}^{\dagger}C_{j+l+1,s}+\text{H.c.})\right\rangle . \tag{3.8}$$

The oscillations in these functions show the existence of a charge-density wave defined on the bonds. Again, one can obtain from this the electron order parameter defined in Eq. (2.5) by taking the

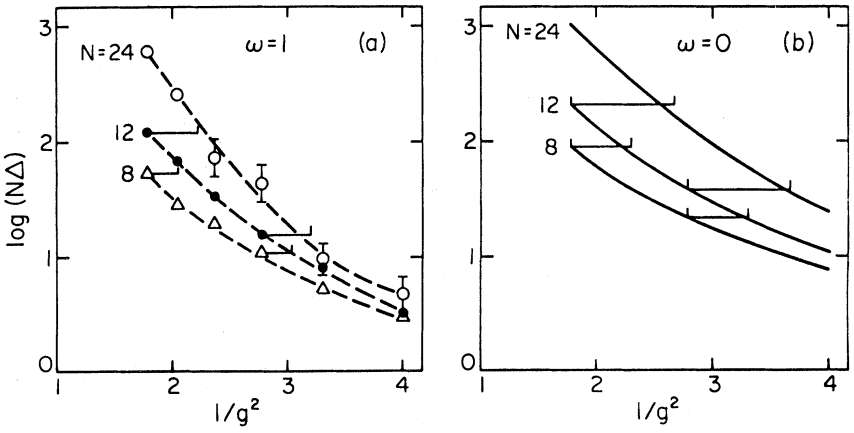

FIG. 13. Finite-size scaling analysis of the SSH model $n=2$. ln of the lattice size times the gap is plotted vs $1/g^2$ for the cases (a) $\omega=1$ and (b) $\omega=0$. Note that the curves are steeper in (a) than in (b). The horizontal bars in (a) and (b) represent the expected distance between the curves in the Gross-Neveu limit [Eq. (3.19b)] and in the static case [Eq. (3.19a)], respectively.

limit of large l.

Figure 9 shows results for the energy as a function of the coupling constant for the case $\omega=1$. We have taken $\beta=20$ here so that this is essentially the ground-state energy. The zero-point energy of the phonon field at zero coupling constant is ω/π, and the numerical results agree with this. The variation of energy with the coupling constant is similar to the one in the static limit, as shown in Fig. 9. (The small discrepancy between the MC and exact static limit results for the electron energy at $g=0$ is due to the finite $\Delta\tau$ used.)

In Fig. 10 we show results for the phonon order-parameter time-correlation function, defined by

$$G_p(\tau)=\langle O_p(\tau)O_p(0)\rangle \ , \tag{3.9}$$

with

$$O_p=\frac{1}{N}\sum_j(-1)^j(q_{j+1}-q_j) \tag{3.10}$$

for the case $\omega=1$ and several values of g on a 24×24 lattice. In the noninteracting case this function is found to be

$$G_p^0(\tau,\omega,M)=\frac{2}{NM\omega}e^{-\omega\tau}\left[1+\frac{1+e^{2\omega\tau}}{e^{\beta\omega}-1}\right] . \tag{3.11}$$

This is drawn as a full line in Fig. 10. For the interacting case we have fitted the correlation function to the form

$$G_p(\tau)=G_p^0(\tau,\bar{\omega},\bar{M})+4m_p^2 \ , \tag{3.12}$$

where the renormalized frequency $\bar{\omega}$ was obtained from the initial slope of the numerical data, and the phonon order parameter m_p and the renormalized mass $\bar{M}$ were obtained by fitting the MC points at $\tau=0$ and $\tau=\beta/2$ to the form (3.12). Even with this three-parameter fit the MC data deviate somewhat from the form equation (3.12) (the dashed lines in Fig. 10), indicating that there are deviations from mean-field theory behavior. Nevertheless, we believe that this is a reasonable way of obtaining the phonon order parameter m_p from data for the correlation functions, especially for small lattices where finite lattice effects are substantial. (A direct measurement of the order parameter is not very accurate because of tunneling between the two degenerate ground states.) We found the value of $\bar{M}$ to be always very close to the bare mass (within 10% for all coupling constants studied) and the renormalized frequency to decrease with the increasing coupling constant, to about $\bar{\omega}\sim 0.57\omega$ for $g=0.75$.

For the case of polyacetylene, Fig. 11 shows the phonon time correlation function and the fit to the MC data, which gives $\bar{\omega}=0.64\omega$. This is in reasonable agreement with the result obtained by Nakahara and Maki[4] for this case ($\bar{\omega}=0.60\omega$).

In Fig. 12 we show results for the phonon order parameter m_p [obtained from Eq. (3.12)] for the case $\omega=1$ and a 24-site lattice, as a function of the coupling constant. We show for comparison also exact results in the static limit for the 24-site lattice and for an infinite lattice. The MC results for $\omega=1$ are always lower than the corresponding $\omega=0$ results for the finite lattice, as expected. It can also be seen from the static results of Fig. 12 that finite-lattice effects are substantial for $g<0.6$ in the 24-site lattice. This happens roughly when $\xi\gtrsim N/4$, where the correlation length ξ is the inverse of the energy gap. We also show in Fig. 12, for comparison, the corresponding results for the spinless case ($n=1$). Although they show a greater reduction than the case $n=2$, no phase transition is apparent if we only look at one size system. We will return to the $n=1$ case later in this section.

In order to determine the analytic behavior of the order parameter or the gap from the numerical data it is essential to take finite-lattice effects into account. We assume that the gap for a finite system of $N=L$ sites, Δ_N, obeys the finite-size scaling hypothesis[27–29]

$$\Delta_N=\frac{1}{N}f(N\Delta_\infty) \ , \tag{3.13}$$

with Δ_∞ the gap for an infinite lattice. To be more precise, N in Eq. (3.13) should be replaced by an effective N, a function of the space and time size of our lattice. However, we will only study systems of varying size with $N=L$ so that the effective N will presumably be proportional to N and we can assume Eq. (3.13) to be valid.

Assume we do a small change in both N and the coupling constant g so that the product $N\Delta_N$ remains unchanged. We have then, from (3.13),

$$0=d(N\Delta_N)=\Delta_\infty f'(N\Delta_\infty)dN + N\frac{d\Delta_\infty}{dg}f'(N\Delta_\infty)dg \ , \tag{3.14}$$

with $f'(x)=df/dx$. We obtain then from (3.14)

$$\frac{dg}{d\ln N}=\left[\frac{d\ln\Delta_\infty}{dg}\right]^{-1} . \tag{3.15}$$

This is the β function of the system. If the gap has the analytic form

$$\Delta_\infty=ce^{-a/g^2} \ , \tag{3.16}$$

then from (3.15)

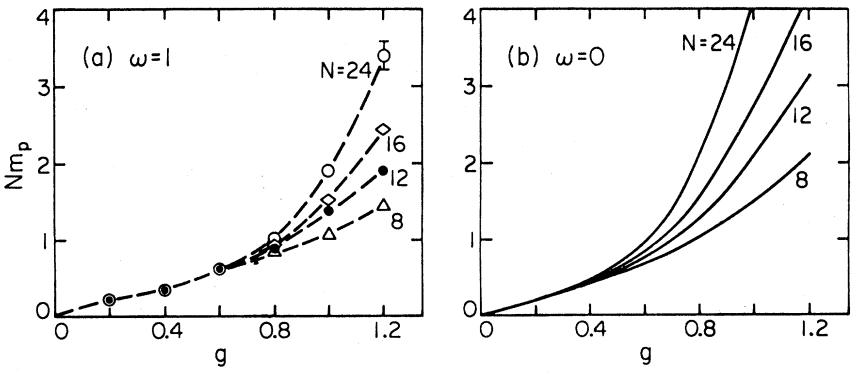

FIG. 14. Finite-size scaling analyses of the SSH model, $n=1$. Lattice size times phonon order parameter is plotted vs g. (a) MC results for the case $\omega=1$. The curves are expected to come together at the transition point. (b) Exact results for the static case, for comparison.

$$\frac{d(1/g^2)}{d\ln N}=\frac{1}{a}\ , \tag{3.17}$$

and we expect $a=\pi/2n$ in the static limit and $a=\pi/2(n-1)$ in the Gross-Neveu regime [Eq. (2.46)]. In practice, we will do finite changes in both N and g. If we have then a system of size N_1 at coupling constant g_1 and a system of size N_2 at coupling g_2 such that

$$N_1\Delta_{N_1}(g_1)=N_2\Delta_{N_2}(g_2)\ , \tag{3.18}$$

we expect

$$\frac{1}{g_1^2}-\frac{1}{g_2^2}=\frac{2n}{\pi}\ln\frac{N_1}{N_2} \tag{3.19a}$$

in the static limit, and

$$\frac{1}{g_1^2}-\frac{1}{g_2^2}=\frac{2(n-1)}{\pi}\ln\frac{N_1}{N_2} \tag{3.19b}$$

in the Gross-Neveu regime. We expect Eq. (3.19) to be valid even in regions where the correlation length is larger than the lattice size.

In Fig. 13 we show $\ln(N\Delta_N)$ vs $1/g^2$ for lattices of size $N=L=24$, $N=L=12$, and $N=L=8$. It is difficult to obtain the gap directly from the MC simulation, so we obtained it from the phonon order parameter through the relation

$$\Delta=4gm_p\ . \tag{3.20}$$

This relation is valid in the static limit and also in perturbation theory to the one-loop order. We show in Fig. 13 MC results for $\omega=1$ (a) and exact results for the static case (b) for comparison. If the lattice was infinite, we would obtain straight lines for the small coupling constant of slope

$$m=\frac{\pi}{2n} \tag{3.21a}$$

in the static case, and

$$m=\frac{\pi}{2(n-1)} \tag{3.21b}$$

if we are in the Gross-Neveu regime. Although the curves in the case $\omega=1$ appear steeper, it is difficult to determine whether (3.21a) or (3.21b) holds. The reason is that for small g, finite-lattice effects set in and the slope becomes smaller than (3.21), while for large g one is outside the scaling regime and the exponential behavior for the gap no longer holds [the slope becomes larger than (3.21b) in the static case]. A better indication of the different behavior is given by measuring the horizontal distance between two curves for different N. In the static case this distance is given by Eq. (3.19a) for small g, and it becomes somewhat smaller for larger g presumably due to irrelevant operators, as seen in Fig. 13(b). In contrast, for the $\omega=1$ case we find the distance for small g to be given approximately by (3.19b), indi-

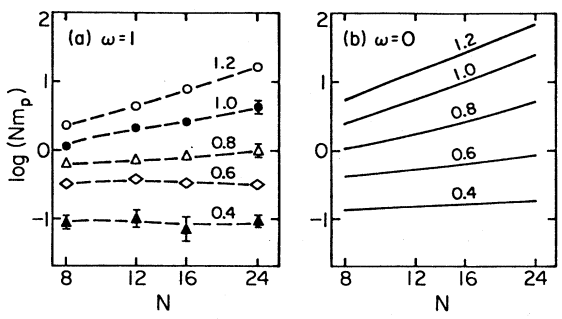

FIG. 15. Lattice size N times phonon order parameter vs N on a log-log plot for the SSH model, $n=1$. (a) MC results for the case $\omega=1$. The lines are expected to become horizontal at the transition point. (b) Exact results for the static case, for comparison.

cating that we are in the Gross Neveu regime. For larger g the distances become *larger* in this case, presumably because the dominant irrelevant operator is produced by the finite mass, and it causes the behavior to approach the $M=\infty$ behavior.

We now discuss briefly the spinless case $n=1$. According to the results of the preceding section, we expect here a transition from an undimerized state at a finite value of the coupling constant g. Again we concentrate on one particular case, $\omega=1$. We computed space and time correlation functions on different size lattices, and obtained the phonon order parameter from the time correlation functions by the procedure discussed previously. We find the electronic charge-density wave to reside always on the bonds. Figure 14 shows the phonon order parameter times the lattice size versus coupling constant. For clarity, we show only the statistical errors of the MC points for $g=1.2$. The relative error in the MC data increases somewhat as g is decreased. Assuming finite-size scaling [Eq. (3.13)] to hold, and if the relation between the gap and the phonon order parameter m_p is given by Eq. (3.20), we expect for m_p on a finite lattice the behavior

$$m_p=\frac{1}{Ng}F(N\Delta_\infty)\ . \tag{3.22}$$

Therefore, curves of Nm_p vs g should come together at the transition point, where Δ_∞ vanishes. From Fig. 14 we see that the curves come together somewhat below $g=0.8$ for $\omega=1$. We also show for comparison the exact results for the static case. Here, even though the transition occurs at $g=0$, the curves appear to come together somewhat below $g=0.4$ because we are dealing with an essential singularity. Much larger lattices would be needed to notice the difference between the curves below $g=0.4$. Nevertheless, the difference between the cases $\omega=1$ and $\omega=0$ is evident, although it is difficult to estimate the precise location of the transition point.

In Fig. 15 we have plotted the same data in a log-log plot versus N for various g. In the ordered region the slope of these curves should approach unity as N becomes larger than the correlation length. But even before that happens, the curves will have a positive slope in the ordered region. At the transition point, Nm_p becomes independent of N. Again from the MC data plotted in this form it appears that the system undergoes a transition for g somewhere between 0.6 and 0.8. Again we show the static results for comparison, which show a positive slope for all g.

While this paper was in the process of being written, we became aware of a longer version of the paper of Campbell and Bishop [Nucl. Phys. B 200 297 (1982)]. In this paper they found, independently from our result, that the polaron disappears from the spectrum as $M\to 0$ in the spin-$\frac{1}{2}$ model via the connection with the Gross-Neveu model.

ACKNOWLEDGMENTS

This work was started at the Institute for Theoretical Physics (ITP), University of California at Santa Barbara. One of us (E.F.) wishes to thank the ITP for its kind hospitality. We would like to thank S. Kivelson, N. Andrei, S. Shenker, W. P. Su, R. Sugar, K. Maki, M. Stone, and particularly D. Scalapino and J. R. Schrieffer for sharing their insights with us. We are grateful to K. Maki and D. Campbell for making their work available to us prior to publication. Additionally, we are grateful to the National Science Foundation for support through Grants Nos. PHY77-27084 and DMR81-17182.

*Permanent address.
†Present address: Department of Physics, University of California, San Diego, La Jolla, CA 92093.

[1]W. P. Su, J. R. Schrieffer, and A. J. Heeger, Phys. Rev. Lett. 42, 1698 (1979).
[2]W. P. Su, J. R. Schrieffer, and A. J. Heeger, Phys. Rev. B 22, 2099 (1980).
[3]H. Takayama, Y. R. Lin-Liu, and K. Maki, Phys. Rev. B 21, 2388 (1980). See also S. A. Brazovskii, Zh. Eksp. Teor. Fiz. 78, 677 (1980) [Sov. Phys.—JETP 51, 342 (1980)].
[4]M. Nakahara and K. Maki, Phys. Rev. B 25, 7789 (1982).
[5]D. K. Campbell and A. R. Bishop, Phys. Rev. B 24, 4859 (1981). See also S. A. Brazovskii and N. Kirova, Zh. Eksp. Teor. Fiz. Pis'ma Red. 33, 6 (1981).
[6]J. E. Hirsch, D. J. Scalapino, R. L. Sugar, and R. Blankenbecler, Phys. Rev. Lett. 47, 1628 (1981); Phys. Rev. B 26, 5033 (1982).
[7]T. Holstein, Ann. Phys. (N.Y.) 8, 325 (1959).
[8]D. Gross and A. Neveu, Phys. Rev. D 10, 3235 (1974).
[9]G. Beni and P. Pincus, J. Chem. Phys. 57, 3531 (1972).
[10]J. E. Hirsch and E. Fradkin, Phys. Rev. Lett. 49, 402 (1982).
[11]This identity is known as a Fierz transformation.
[12]M. P. M. den Nijs, Phys. Rev. B 23, 6111 (1981).
[13]N. D. Mermin and H. Wagner, Phys. Rev. Lett. 17, 1133 (1966).
[14]E. Witten, Nucl. Phys. B 142, 285 (1978).
[15]E. Lieb and D. C. Mattis, J. Math. Phys. 6, 304 (1965).
[16]S. Coleman, Phys. Rev. D 11, 2088 (1975).
[17]S. Mandelstam, Phys. Rev. D 11, 3026 (1975).
[18]A. Luther, Phys. Rev. B 14, 2153 (1975).

[19]M. Kosterlitz, J. Phys. C 7, 1046 (1974).
[20]P. B. Wiegmann, J. Phys. C 11, 1583 (1978).
[21]D. J. Amit, Y. Goldschmidt, and G. Grinstein, J. Phys. A 13, 585 (1980).
[22]S. Raby and A. Ukawa, Phys. Rev. D 18, 1154 (1978).
[23]R. Dashen, B. Hasslacher, and A. Neveu, Phys. Rev. D 12, 2443 (1975).
[24]A. B. Zamolodchikov and A. B. Zamolodchikov, Ann. Phys. (N.Y.) 120, 253 (1979).
[25]M. Karowski and H. J. Thun, Nucl. Phys. B 190, 61 (1981).
[26]W. P. Su, Solid State Commun. 42, 497 (1982).
[27]M. E. Fisher and M. N. Barber, Phys. Rev. Lett. 28, 1516 (1972).
[28]C. J. Hamer and M. N. Barber, J. Phys. A 14, 241 (1981).
[29]H. H. Roomany and H. W. Wyld, Phys. Rev. D 21, 3341 (1980).